

AN ASCA STUDY OF THE HIGH LUMINOSITY SNR G349.7+0.2

PATRICK SLANE¹, YANG CHEN², JASMINA S. LAZENDIC¹, AND JOHN P. HUGHES³*Accepted for Publication in The Astrophysical Journal*

ABSTRACT

We present *ASCA* observations of supernova remnant (SNR) G349.7+0.2. The remnant has an irregular shell morphology and is interacting with a molecular cloud, evident from the presence of OH(1720 MHz) masers and shocked molecular gas. The X-ray morphology is consistent with that at radio wavelengths, with a distinct enhancement in the south. The X-ray emission from the SNR is well described by a model of a thermal plasma which has yet to reach ionization equilibrium. The hydrogen column of $\sim 6.0 \times 10^{22} \text{ cm}^{-2}$ is consistent with the large distance to the remnant of ~ 22 kpc estimated from the maser velocities. We derive an X-ray luminosity of $L_x(0.5\text{-}10.0\text{ keV}) = 1.8 \times 10^{37} d_{22}^2 \text{ erg s}^{-1}$, which makes G349.7+0.2 one of the most X-ray luminous shell-type SNRs known in the Galaxy. The age of the remnant is estimated to be ~ 2800 yrs. The ambient density and pressure conditions appear similar to those inferred for luminous compact SNRs found in starburst regions of other galaxies, and provides support for the notion that these may be the result of SNR evolution in the vicinity of dense molecular clouds.

Subject headings: radiation mechanisms: thermal — supernova remnants: individual: G349.7+0.2 — X-rays: ISM

1. INTRODUCTION

Because massive stars evolve quickly, they are often not far from their birth sites when they expire. The result is that many of the supernova remnants (SNRs) produced in the explosive events that mark the endpoint of stellar evolution for these stars are located near the molecular cloud complexes from which the progenitors emerged. The initial expansion of such an SNR is likely to proceed rather effortlessly as the progenitor star has generally sculpted a cavity in the ambient medium by virtue of a strong wind (Chevalier 1999). Eventually the blast wave must contend with the cavity walls, however, and when the cavity resides in a dense molecular cloud the resulting interaction reveals itself spectacularly in X-rays (Chevalier & Liang 1989). The remnant sweeps up massive amounts of material and heats it to X-ray emitting temperatures while seeding the cloud with metals synthesized in the supernova explosion. Such young SNRs encountering dense material can transform a large amount of their kinetic energy into radiation, appearing as bright (radio and X-ray) emission sources, often with irregular morphologies. They may be representative of a larger class of compact SNRs identified as bright radio sources in starburst regions of other galaxies (e.g. Kronberg, Biermann, & Schwab 1985; Antonucci & Ulvestad 1988; and Smith et al. 1998). Chevalier & Fransson (2001) have proposed that these sources represent SNRs that have evolved in the high density interclump medium of molecular clouds, and that a similar population that has escaped such high density regions is responsible for driving galactic winds in the host galaxies.

A good example of this type of SNR is N132D in the Large Magellanic Cloud (LMC). It is a luminous ($\sim 5 \times 10^{37} \text{ erg s}^{-1}$ in X-ray band) small diameter SNR ($\sim 44'' = 11.7 \text{ pc}$) that is evolving into a cavity wall on the edge of a molecular cloud (Hughes 1987, Banas et al. 1997). The X-ray emitting material comprises several hundred solar masses and the overall abundances are characteristic of the LMC interstellar material,

implying that the bulk of the emission is from swept-up material. However, optical spectra (Danziger & Dennefeld 1976) show that N132D is an oxygen rich SNR whose abundances are consistent with a $\sim 20 M_{\odot}$ progenitor (Blair, Raymond, & Long 1994), and high resolution X-ray spectral studies show the presence of an ejecta component as well (Hwang et al. 1993, Behar et al. 2001) indicating that N132D is a relatively young SNR; the large amount of swept-up material, as well as the high X-ray luminosity, are the result of an explosion in the high density surroundings of a molecular cloud.

G349.7+0.2 appears in some ways to be a Galactic counterpart to N132D. It is an SNR with a small angular size ($r \sim 1$ arcmin) and the third highest radio surface brightness next to Cas A and the Crab Nebula. Its nonthermal radio emission ($\alpha_r \simeq -0.5$) and roughly circular morphology, classifies it as a shell-type SNR (Shaver et al. 1985). However, it has an emission peak near the southeastern edge rather than a prominent limb-brightened structure and central cavity typical of shell-type remnants. The early H I absorption measurements showed that G349.7+0.2 lies beyond the tangent point, with the kinematic distance in the range $13.7 < d < 23 \text{ kpc}$ (Caswell et al. 1975). OH(1720 MHz) masers have been recently found interior to G349.7+0.2 with radial velocities $\sim +16 \text{ km s}^{-1}$ indicating a kinematic distance $d \approx 22.4 \text{ kpc}$ (Frail et al. 1996), for which the SNR radius is 6.4 kpc. This maser emission, detected in about 10% of the Galactic SNRs, has been recognized as a signpost of SNR interactions with molecular clouds (see Koralesky et al. 1998 and references therein; also Lockett, Gauthier & Elitzur 1999). The masers are located along the radio ridge extending from the southern emission peak to the north. CO observations toward G349.7+0.2 revealed a molecular cloud associated with the SNR, and with the masers (Reynoso & Mangum 2000, Reynoso & Mangum 2001) which have been produced by shocks from the expanding SNR blast wave (Lazendic et al. 2002).

¹ Harvard-Smithsonian Center for Astrophysics, 60 Garden Street, Cambridge, MA 02138

² Department of Astronomy, Nanjing University, Nanjing 210093, P. R. China

³ Department of Physics and Astronomy, Rutgers, The State University of New Jersey, Piscataway, NJ 08854-8019

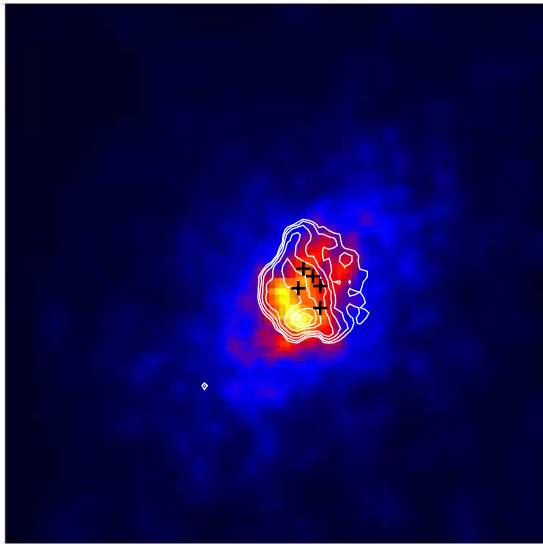


FIG. 1.— The broad band (1.0-10.0 keV) ASCA SIS image of G349.7+0.2. Contours are from the ATCA 18-cm continuum image, with levels at 10, 17, 33, 66, 132, 198 and 264 mJ beam⁻¹. Crosses mark OH(1720 MHz) maser positions. Comparison of *Chandra* and ASCA

G349.7+0.2 went undetected in the *ROSAT* all-sky survey. As we show below, this is the result of the high interstellar absorption of soft X-ray photons. The remnant was detected in the ASCA Galactic plane survey (Yamauchi et al. 1998), and we have followed up this detection with a 60 ks observation that was obtained in two pointings.

2. ASCA DATA

The pointed observations of G349.7+0.2 were carried out with ASCA satellite on 16–17 March 1998 (25 ks) and 19–20 March 1999 (36 ks) with the solid-state imaging spectrometer (SIS) and the gas imaging spectrometer (GIS). The SIS observations were performed in 1-CCD mode to provide the best spectral resolution. The single-chip field of view provides sufficient sky coverage for independent background subtraction. The data were screened according to standard procedures for GIS and SIS data, resulting in roughly 48(53) ks of good exposure time with $\sim 6500(12000)$ SIS(GIS) events from the SNR in each camera.

2.1. X-ray Image of G349.7+0.2

In Figure 1 we present the exposure-corrected 1–10 keV X-ray image of G349.7+0.2 produced by merging the SIS0 and SIS1 maps. Each map from the two exposures was adaptively smoothed using a Gaussian kernel with a minimum of 50 counts in each smoothing element. Inspection of images in different energy bands show no obvious variations in morphology. However, the modest angular resolution of ASCA limits our ability to detect variations on scales below $\sim 2'$. The radio image, shown as contours in Figure 1, is characterized by a distinct brightness enhancement along the southwestern limb, where the remnant is interacting with a molecular cloud. The X-ray brightness is enhanced in this region as well, and the overall morphology is similar to that observed in the radio. The larger apparent size in X-rays, with emission extending beyond the radio shell, is

⁴ Uncertainties here and throughout the paper represent 90% confidence intervals

largely an artifact of the broad angular response of the X-ray telescope. In the analysis presented below we use the radio size of the SNR to estimate its radius. Higher resolution X-ray observations will be required to fully explore the distribution of the X-ray emitting gas.

2.2. Spectral Analysis

To investigate the spectrum of G349.7+0.2, we used both GIS and SIS data. For each GIS detector (GIS2 and GIS3), data from the two observations were merged to form a single spectrum. Based on the centroids of the spectral lines, a gain adjustment of $\sim 3\%$ was required, consistent with known uncertainties in the GIS calibration. The spectra were extracted from a circular region with a radius $6''.8$, centered at R.A. = $17^h18^m03^s$, decl. = $-37^\circ26'07''$ (J2000). The spectra from the four SIS data sets were extracted from a region with the same center, but with a radius of $2''.8$. For both the SIS and GIS, background spectra were extracted from the outer regions of the detectors. Spectra were re-grouped to include at least 25 net counts per bin. Because of resolution changes between the two observations, data from the same cameras (SIS0 and SIS1) were not combined. Our spectral analyses were thus based on simultaneous fitting of two GIS spectra and four SIS spectra.

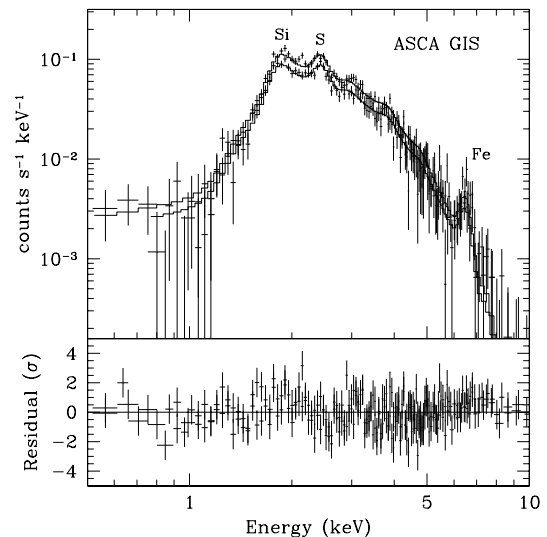


FIG. 2.— ASCA GIS spectra and residuals for the NEI fit described in the text.

As illustrated in Figure 2, the spectrum is dominated by line features from Si, S, and Fe-K. There is no emission below ~ 1.5 keV, indicating a large value of line-of-sight hydrogen column density N_H . The centroids of the distinct line features were determined by fitting Gaussian profiles to these regions of the spectra. We obtain $1.86^{+0.02}_{-0.01}$ keV for Si He α , $2.42^{+0.02}_{-0.01}$ keV for S He α , and $6.53^{+0.09}_{-0.10}$ keV for Fe K α . The broadband spectrum can be modeled adequately ($\chi^2_\nu = 1.18$) as an optically thin thermal plasma ($kT_x = 1.05 \pm 0.03$ keV) in collisional ionization equilibrium (CIE; Raymond & Smith 1977) modified by interstellar absorption (Morrison & McCammon 1983) of $N_H = (5.7 \pm 0.1) \times 10^{22}$ cm⁻², and with normal solar abundances⁴. This indicates that the X-ray emitting plasma of G349.7+0.2 is dominated by the swept-up interstellar material,

TABLE 1

RESULTS FROM CIE MODEL (RAYMOND & SMITH 1977) FIT TO 2 GIS AND 4 SIS DATA SETS, WITH THE 90% CONFIDENCE RANGES.

Parameter	CEI	Value NEI	VPSHOCK
$fn_{en_H}V/(d/22\text{kpc})^2$ (10^{59}cm^{-3})	8.8 7.0	10.2	
T_x (keV)	$1.05^{+0.02}_{-0.03}$	$1.26^{+0.03}_{-0.05}$	1.12 ± 0.03
N_H (10^{22}cm^{-2})	5.7 ± 0.1	5.8 ± 0.1	5.9 ± 0.1
n_{et} ($10^{11}\text{cm}^{-3}\text{s}$)		$1.7^{+0.5}_{-0.3}$	$6.5^{+2.9a}_{-1.8}$
$F(0.5\text{-}10\text{keV})$ ($\text{erg cm}^{-2}\text{s}^{-1}$)	7.0×10^{-12}	7.1×10^{-12}	7.2×10^{-12}
$F_{\text{unabs}}(0.5\text{-}10\text{keV})$ ($\text{erg cm}^{-2}\text{s}^{-1}$)	1.4×10^{-10}	1.7×10^{-10}	2.8×10^{-10}
$\chi^2/\text{d.o.f.}$	708.5/599	669.6/598	661.0/598

a) Represents maximum value of continuous range in VPSHOCK model

with no significant evidence of emission from the supernova ejecta.

An improved fit ($\Delta\chi^2 = 39.1$ for one additional fit parameter) is obtained with a single-temperature non-equilibrium ionization (NEI) model (Hughes & Singh 1994) with $kT = 1.26 \pm 0.05$ keV and an ionization timescale $n_{et} = (1.7 \pm 0.4) \times 10^{11} \text{ s cm}^{-3}$, indicating that the plasma is still ionizing. A single-temperature plane-parallel shock model (VPSHOCK, Borkowski et al. 2001) yields an equally good fit with similar parameters. Here the ionization parameter is allowed to vary from zero to a fit-determined maximum value of $6.5^{2.9}_{1.8} \times 10^{11} \text{ s cm}^{-3}$; this range is consistent with the average value determined in the single ionization timescale model. No significant contribution of a power law component is found. The spectral fit results are tabulated in Table 1.

The hydrogen column $N_H \sim 6 \times 10^{22} \text{ cm}^{-2}$ confirms a substantial absorption of the soft emission (< 1.5 keV) and is consistent with a very large distance. The corresponding X-ray luminosity (using the NEI fit) is $L_x(0.5\text{-}10\text{keV}) = 1.8 \times 10^{37} d_{22}^2 \text{ erg s}^{-1}$, which makes G349.7+0.2 one of the most X-ray luminous Galactic SNRs known, rivaling even the young ejecta-dominated remnant Cas A. The radius for G349.7+0.2 is ~ 1 arcmin, for which its dimensional size is $r_s \sim 6.4 d_{22} \text{ pc}$. The volume emission measure produces a mean hydrogen density $n_H \sim 4.2 f^{-1/2} d_{22}^{-1/2} \text{ cm}^{-3}$ (assuming $n_e \approx 1.2 n_H$), where f is the volume filling factor (i.e. $V = \frac{4}{3} \pi R^3 f$ is the volume of the X-ray emitting region, where R is the SNR radius); for a Sedov-phase SNR, $f = 0.25$ (Sedov 1959). The X-ray emitting mass $M_x = 1.4 n_H m_H f V$ is $\sim 160 f^{1/2} d_{22}^{5/2} M_\odot$.

Assuming G349.7+0.2 is in the adiabatic phase of evolution (Sedov 1959), the post-shock temperature is $kT_s \approx 0.77 kT_x \sim 1$ keV ($T_x \approx 1.2 \times 10^7$ K). The blast wave velocity is accordingly $v_s = (16 kT_s / 3 \mu m_H)^{1/2} \sim 900 \text{ km s}^{-1}$ (where the mean atomic weight $\mu = 0.604$). Thus, an estimate of the age of the remnant is $t = 2r_s / 5v_s \sim 2800 d_{22} \text{ yr}$. This estimate results directly from the X-ray temperature fit and should be more reliable than the $1.4 \times 10^4 \text{ yr}$ Reynoso & Mangum (2001) obtained using an assumed explosion energy and adopting a rough estimate of the cloud density as the remnant's ambient density. The explosion energy is approximately $E = 1.12 \times 10^{-24} n_0 (r_s^5 / t^2) \sim 5 \times 10^{50} f^{-1/2} d_{22}^{5/2} \text{ erg}$. We note, however, that the electron temperature in the shocked gas (i.e. the temperature inferred from X-ray spectral fits) lags the ion temperature, while it is the latter that determines the SNR dynamics. If full temperature equilibrium has not yet occurred in G349.7+0.2, so that the shock

velocity is actually higher than that indicated by the electron temperature, then the age given above is an overestimate while the explosion energy is an underestimate.

3. DISCUSSION

The normal abundances and large X-ray emitting mass found in G349.7+0.2 indicate that the gas is dominated by swept-up interstellar material, which is consistent with the SNR location near the molecular cloud. The maximum radio and X-ray brightness occurs in a region where the SNR shell is encountering a molecular cloud with a radius of $24''$ (2.6 pc), a mass of $1.2 \times 10^4 M_\odot$, and a gas density of $\sim 10^4 \text{ cm}^{-3}$ (Reynoso & Mangum 2001). This cloud, as well as G349.7+0.2, lies along a large CO filament (Figure 3). Beyond the positional coincidence, an on-going interaction between G349.7+0.2 and the molecular cloud is implied by the presence of OH(1720 MHz) masers and the detection of shocked molecular gas. The OH(1720 MHz) maser spots detected from G349.7+0.2 (Frail et al. 1996) are attributed to C-shock collisional excitation in the clumpy molecular clouds, with cloud temperature and density conditions $50 \leq T \leq 125$ K and $n_{H_2} \sim 10^5 \text{ cm}^{-3}$ (Lockett, Gauthier & Elitzur 1999). Molecular-line observations toward the maser region in G349.7+0.2 confirm the presence of shocked molecular gas with density $10^5 - 10^6 \text{ cm}^{-3}$ and temperature > 40 K (Lazendic et al. 2002).

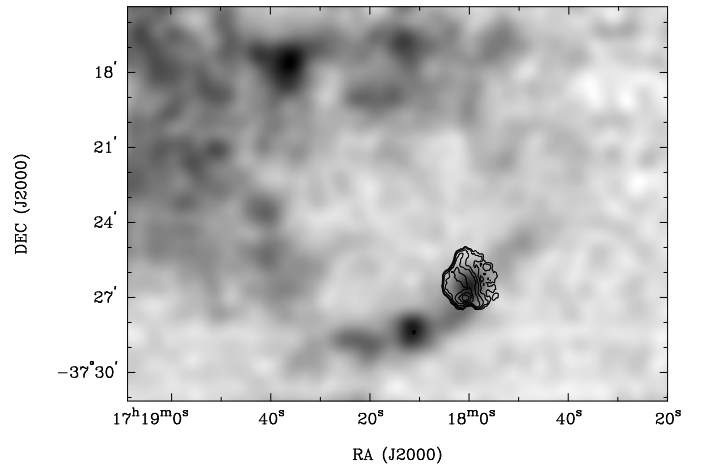


FIG. 3.— Velocity-integrated CO 1-0 image of the region around G349.7+0.2 from Reynoso & Mangum (2001) overlaid with the radio contours. The greyscale range is from -6 K to 51 K km s^{-1} . The contour levels are same as in Fig. 1.

The adjacency of G349.7+0.2 to dense molecular clouds sug-

gests that its progenitor was a massive star that did not move significantly from its birthplace prior to explosion. Early type (O4 – B0) massive stars, during their main sequence lifetime, will photoevaporate nearby clouds and homogenize a region of radius $R_h = 56n_m^{-0.3}$ pc, where n_m denotes the mean medium density (McKee, van Buren, & Lazareff 1984). Since the maser clouds exist at $r \lesssim 6.4d_{22}$ pc, the medium density should satisfy $n_m \gtrsim 1.4 \times 10^3 d_{22}^{3.3} \text{ cm}^{-3}$ if the progenitor was earlier than B0. This mean density is consistent with that expected in the molecular clouds which harbor OH(1720 MHz) masers.

The thermal pressure of the hot X-ray shell is $P_{\text{sh}} \approx 2.3n_H kT_s \sim 1.6 \times 10^{-8} f^{-1/2} d_{22}^{-1/2} \text{ erg cm}^{-3}$. This is higher than the thermal gas pressure in the maser portions of the shocked clumps, where $P_{\text{cl}} = n_{\text{H}_2} kT \sim 9 \times 10^{-9} \text{ erg cm}^{-3}$, using the upper range of n_{H_2} and kT allowable for the production of strong masers (see above). Moreover, if electron-ion equilibration has not yet been achieved in the X-ray shell, the pressure in this gas is even higher. The discrepancy implies that there must be a contribution from the magnetic pressure and/or cosmic ray pressure in the shocked molecular gas. The strength of the line-of-sight magnetic field determined using Zeeman splitting of the OH(1720 MHz) line is $B_\theta = 3.5 \pm 0.5 \times 10^{-4} \text{ G}$ (Brogan et al. 2000), where θ is the angle between the magnetic field vector and the line of sight. Similar measurements in other remnants have demonstrated that the B_θ values are not confined just to the maser locations but represent a global measurement of the magnetic field in the post-shock molecular gas (Claussen et al. 1997). This yields a magnetic pressure $P_{\text{mag}} = B_\theta^2/8\pi \approx 5 \times 10^{-9} \text{ erg cm}^{-3}$ which still falls short of the pressure in the shell. Further, if the masers are saturated, the true maser field may be as much as a factor of 5 lower than that inferred from Zeeman splitting (Brogan et al. 2000). This would appear to suggest either a slight overpressure in the SNR shell or a non-negligible cosmic ray pressure component in the molecular gas. The latter would appear plausible in that the radiative shock in the molecular gas will suffer rapid cooling and compression, resulting in an increase in the density and cosmic ray pressure.

The overall properties of G349.7+0.2 are similar to those proposed by Chevalier & Fransson (2001) to explain the nature of compact SNRs in starburst galaxies such as M82. The high ambient density associated with the presence of molecular clouds leads to rapid evolution of the SNR and a short-lived period of very high luminosity, after which the shell becomes radiative and the SNR cools rapidly. The radio emission from such remnants persists for longer than the X-ray emission, which is consistent with the fact that those in starburst galaxies are primarily

recognized based on their radio luminosity. G349.7+0.2 is still dynamically young enough to produce a significant flux of X-rays as well. The density, age, and luminosity inferred above are in good agreement with the model predictions of Chevalier & Fransson (2001); G349.7+0.2 appears to be several thousand years old and has evolved in the vicinity of a complex of molecular clouds, apparently encountering gas with an average density of order 5 cm^{-3} , and driving a shock into more dense adjacent molecular gas, thereby exciting OH maser emission. If this scenario is indeed correct, then the region in which the SNR shell has gone radiative should be accompanied by an HI shell. High resolution mapping of this region in HI is thus of considerable interest.

4. CONCLUSIONS

The ASCA SIS and GIS spectra of the SNR G349.7+0.2 are well described by a model for a somewhat underionized, optically thin, thermal plasma. The spectral analysis confirms that it is a distant, young SNR that has swept up considerable interstellar material, consistent with the picture that G349.7+0.2 is interacting with an adjacent molecular cloud that is observed in CO. Velocity measures based on OH masers produced by this cloud interaction yield a distance to the remnant, based upon which we conclude that G349.7+0.2 is one of the most X-ray luminous shell-type SNRs known in the Galaxy. Combined with its high radio luminosity, this G349.7+0.2 appears to be a young analog of the bright SNRs observed in starburst galaxies, many of which have evolved in such high density/pressure regions that they have already become radiative and X-ray faint. We note that N132D, a similar SNR in the LMC, shows evidence for ejecta in its X-ray emission. Given the relatively young age, it may be that such a component persists in G349.7+0.2 as well, but is dominated by the emission from swept up material. The high column density to the SNR rules out any opportunity to detect oxygen ejecta, but evidence for Fe-K ejecta is also seen in N132D, and could be observable in G349.7+0.2 with higher sensitivity measurements. Future high resolution X-ray studies, already planned, offer the possibility to search for such a component.

We thank Dick Edgar and John Raymond for helpful discussions related to this study, as well as the referee, Rob Petre, for his careful review of the text. Y.C. acknowledges support from CNSF grant 1007003 and grant NKBRSF-G19990754 of China Ministry of Science and Technology. This work was also supported, in part, by NASA contract NAS8-39073 and grant NAG5-8354 (POS).

REFERENCES

- Antonucci, R. R. J. & Ulvestad, J. S. 1988, *ApJ*, 330, L97
 Banas, K. R., Hughes, J. P., Bronfman, L., & Nyman, L.-A. 1997, *ApJ*, 480, 607
 Behar, E., Rasmussen, A. P., Griffiths, R. G., Dennerl, K., Audard, M., Aschenbach, B., & Brinkman, A. C. 2001, *A&A*, 365, L242
 Borkowski, K. J., Lyerly, W. J., & Reynolds, S. P. 2001, *ApJ*, 548, 820
 Brogan, C. L., Frail, D. A., Goss, W. M., & Troland, T. H. 2000, *ApJ*, 537, 875
 Caswell, J. L., Murray, J. D., Roger, R. S., Cole, D. J., & Cooke, D. J. 1975, *A&A*, 45, 239
 Chevalier, R. A. 1999, *ApJ*, 511, 798
 Chevalier, R. A. & Fransson, C. 2002, *ApJ*, 558, L27
 Chevalier, R. A. & Liang, E. P. 1989, *ApJ*, 344, 332
 Claussen, M. J., Frail, D. A., Goss, W. M., & Gaume, R. A. 1997, *ApJ*, 489, 143
 Frail, D. A., Goss, W. M., Reynoso, E. M., Giacani, E. B., Green, A. J. & Otrupcek, R. 1996, *AJ*, 111, 1651
 Hughes, J. P. 1987, *ApJ*, 314, 103
 Hughes, J. P. & Singh, K. P. 1994, *ApJ*, 422, 126
 Hwang, U., Hughes, J. P., Canizares, C. R., & Markert, T. H. 1993, *ApJ*, 414, 219
 Koralesky, B., Frail, D. A., Goss, W. M., Claussen, M. J., & Green, A. J. 1998, *AJ*, 116, 1323
 Kronberg, P. P., Biermann, P., & Schwab, F. R. 1985, *ApJ*, 291, 693
 Lazendic, J. S., Wardle, M., Green, A. J., Whiteoak, J. B., & Burton, M. G. 2002, to appear in "Neutron Stars in Supernova Remnants" (ASP Conference Proceedings), eds P. O. Slane and B. M. Gaensler
 Lockett, P., Gauthier, E. & Elitzur, M. 1999, *ApJ*, 511, 235
 McKee, C. F., van Buren, D., & Lazareff, B. 1984, *ApJ*, 278, L115
 Morrison, R. & McCammon, D. 1983, *ApJ*, 270, 119
 Murray, S. S., Fabbiano, G., Epstein, A., Giacconi, R., & Fabian, A. C. 1979, *ApJ*, 234, L69
 Raymond, J. C. & Smith, B. W. 1977, *ApJS*, 35, 419

- Reynoso, E. M. & Mangum, J. G. 2000, ApJ, 545, 874
Reynoso, E. M. & Mangum, J. G. 2001, AJ, 121, 347
Sedov, L. I. 1959, *Similarity and Dimensional Methods in Mechanics*, New York: Academic Press, 1959
Shaver, P. A., Salter, C. J., Patnaik, A. R., van Gorkom, J. H., & Hunt, G. C. 1985, Nature, 313, 113
Smith, H. E., Lonsdale, C. J., Lonsdale, C. J., & Diamond, P. J. 1998, ApJ, 493, L17
Yamauchi, S., Koyama, K., Kinugasa, K., Torii, K., Nishiuchi, M., Kosuga, T., & Kamata, Y. 1998, Astronomische Nachrichten, 319, 111